

Fig. 11. This is the BL97 published location of N300-S1 (α 00 54 19.21, δ -37 37 23.96) as found on the BL97 images (Image D) with 2MASS calibrated astrometry. The $H\alpha$ image is on the left and the $[S II]$ image is on the right. The pandas on both images are centered on the published coordinates for N300-S16, as guided by the 2MASS calibrated WCS for these images. The inner circle of the panda is $5''.1$ in diameter (52 pc) and the outer circle is $10''.2$ (104 pc) in diameter. The color scale is AIPS0, Zoom = 4, Scale = ZScale, Squared.

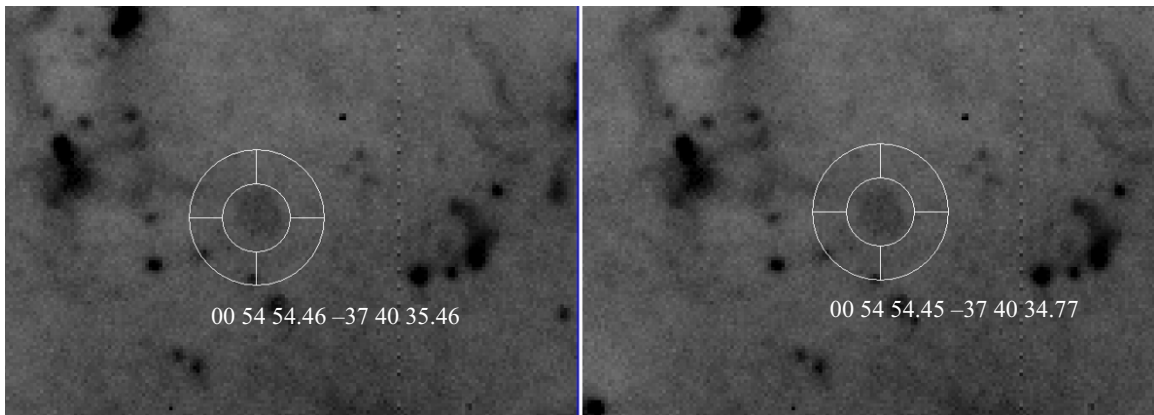


Fig. 12. This is the BL97 location of N300-S16. The $H\alpha$ G image is shown on both the left and right with north up and east to the left. The inner circle of the pandas is $4''$. On the left is the reported position of NS16 (BL97) and on the right is the apparent center of the assumed (probable) image of the SNR candidate on the image. The astrometry error is within the typical seeing of two-meter class telescopes and within the reported seeing conditions for the observation.

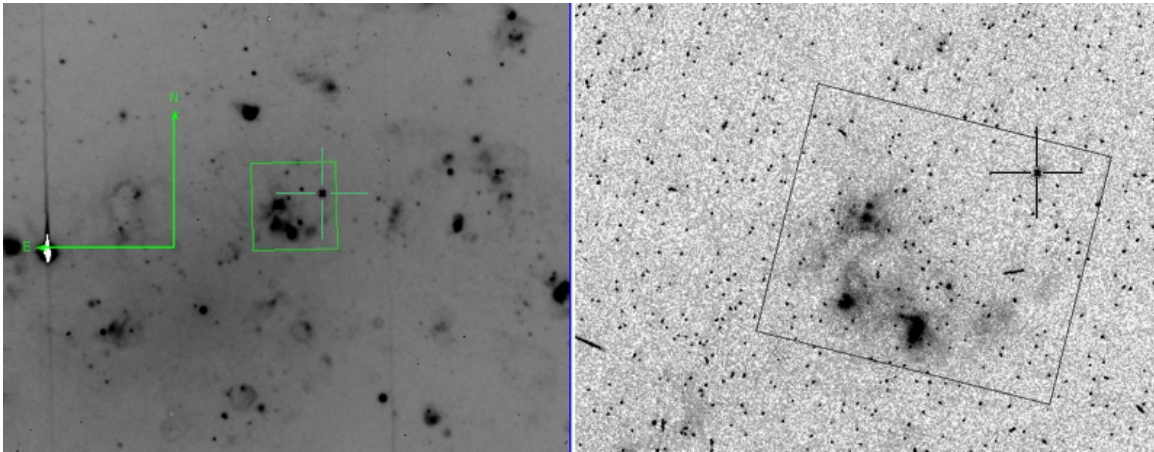


Fig. 13. A comparison of the position of a bright star in BL97 G $H\alpha$ image and the HST image `u6713709r_drz.fits`. The images are both rotated to show north as up, east to the left. The boxes show a set of H II regions used to help identify the star and the selected star is marked with a cross. The measured difference in position is shown in Table 9.

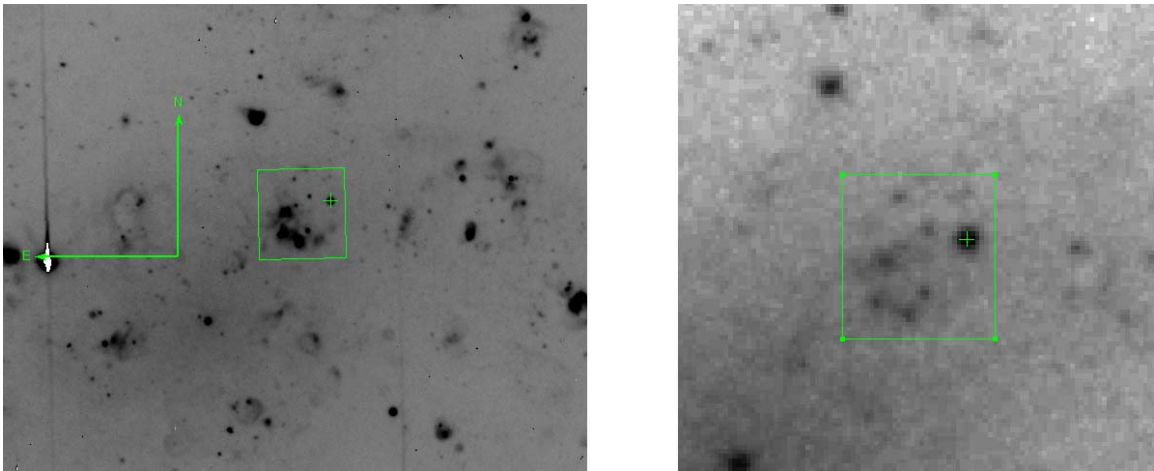


Fig. 14. A comparison of the position of a bright star in BL97 G $H\alpha$ image and a DSS2-Red image containing the same H II regions. The image frames are both rotated to show north as up, east to the left. The boxes show a set of H II regions used to help identify the star and the selected star is marked with a small cross. The measured difference in position is shown in Table 9.

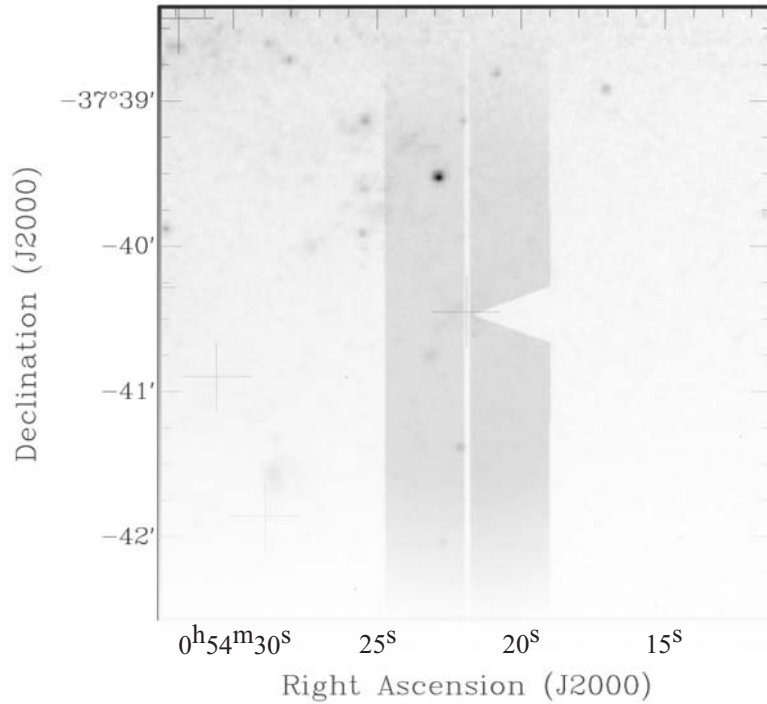


Fig. 15. The DBS slit camera image laid on top of the MWF11 finding map for BL97 candidate N300-S2. The circled objects are those which were used for the alignment of the two images. The pointing was exact but there is a significant difference between the measured $[\text{S II}]:\text{H}\alpha$: BL97 = 0.49 and MWF11 = 0.72 ± 0.39 . The large error in flux estimate also allows this object to be below the $[\text{S II}]:\text{H}\alpha$ critical value.

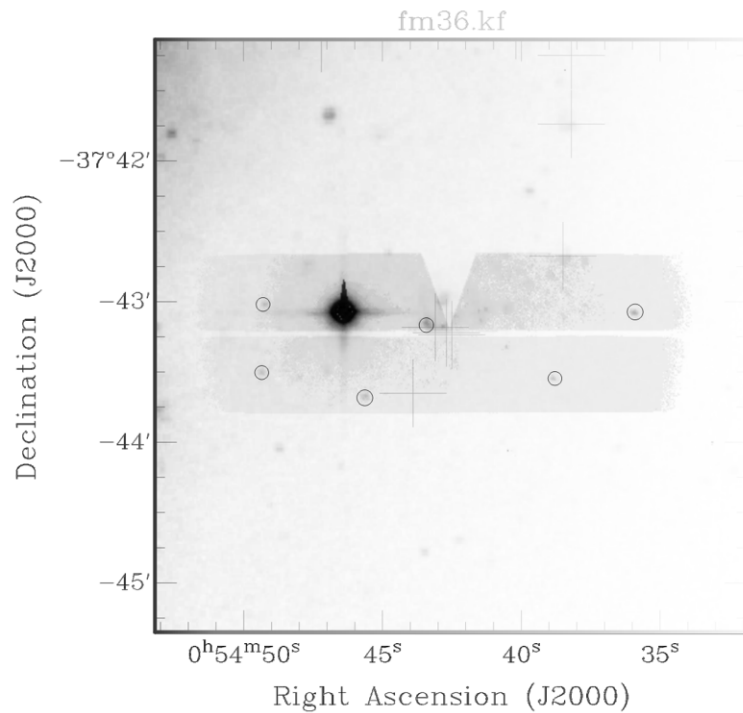


Fig. 16. The DBS slit camera image laid on top of the MWF11 finding map for BL97 candidate N300-S11 (lower right cross). The circled objects are those which were used for the alignment of the two images. In this case there is significant source confusion. See text.

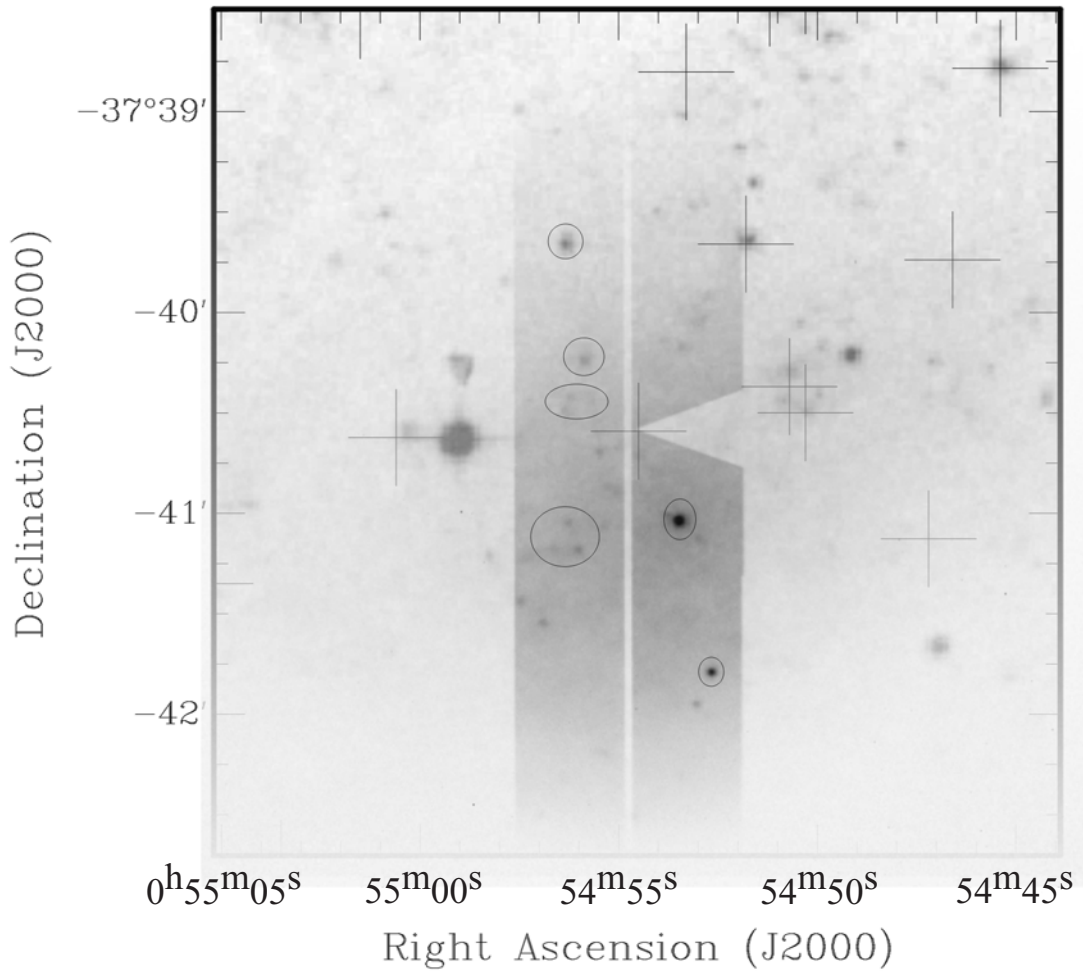


Fig. 17. The DBS slit camera image laid on top of the MWF11 finding map for BL97 candidate N300-S16. The circled objects are those which were used for the alignment of the two images. Due to pointing error the slit was not well aligned with the reported position of N300-S16 but a $[\text{S II}]:\text{H}\alpha$ of 0.70 (BL97) or 0.94 ± 0.06 (MWF11) was measured.

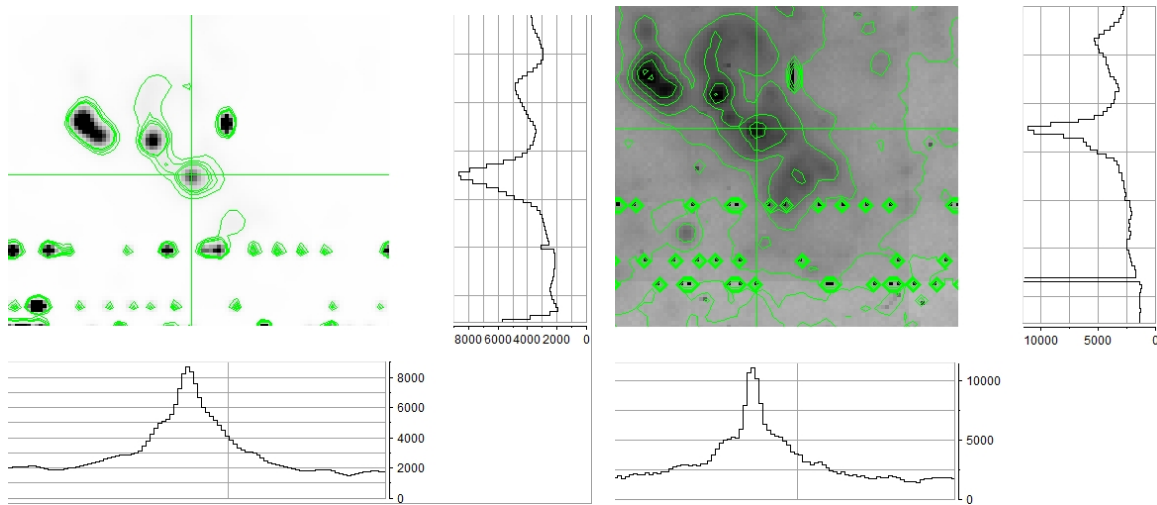


Fig. 18. Stacked BL97 $H\alpha$ images of the SNR candidates. The left and right renditions differ in intensity scale, zoom level and contour line count. The profiles of the image stack for x (E-W) and y (N-S) axes are shown below and to the right, respectively. The lines across the rendition (crosshairs) indicate which CCD row (x) and column (y) are displayed in the profiles. These renditions were created with DS9 after stacking the SNR images with SBIG's CCDOps software.

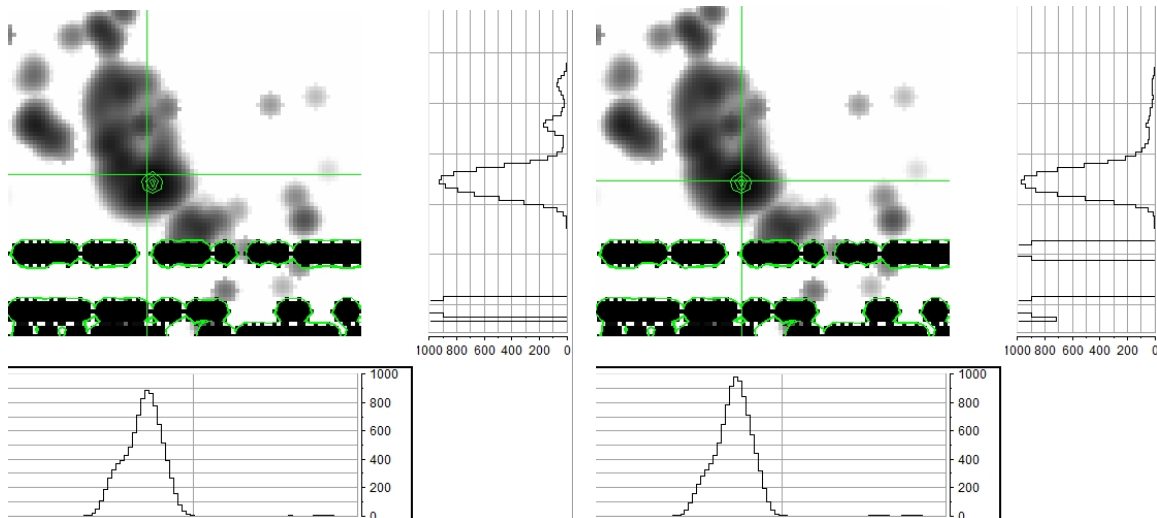


Fig. 19. Stacked $[S II]$ images of the BL97 SNR candidates. The left and right renditions differ in the takeoff location of the profiles. The left rendition's profiles are based on the position of the SNR candidate. The right rendition's profiles are based on the pixel with the maximum count. In each rendition, the profiles of the image stack for x (E-W) and y (N-S) axes are shown below and to the right, respectively. The lines (crosshairs) across the rendition indicate which CCD row (x) and column (y) are displayed in the profiles. These rendition were created with DS9 after stacking the SNR images with SBIG's CCDOps software.

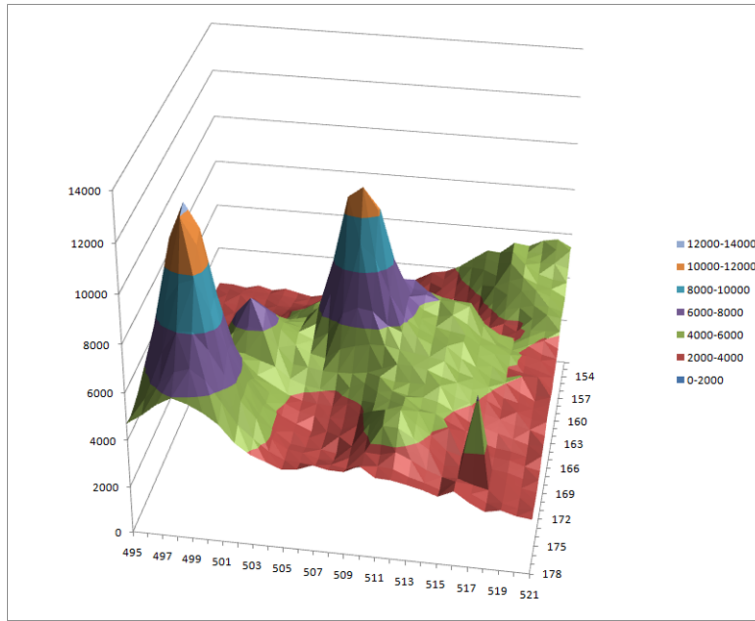


Fig. 20. This is a 27×27 pixel (110×110 pc) surface plot of the central SNR location of the stacked $H\alpha$ images shown in Fig. 18. The data values of the central 9×9 region is shown in Table 10. A plot of the peak along the x -axis (E-W) at y -axis (N-S) pixel row 165 is shown in Fig. 21.

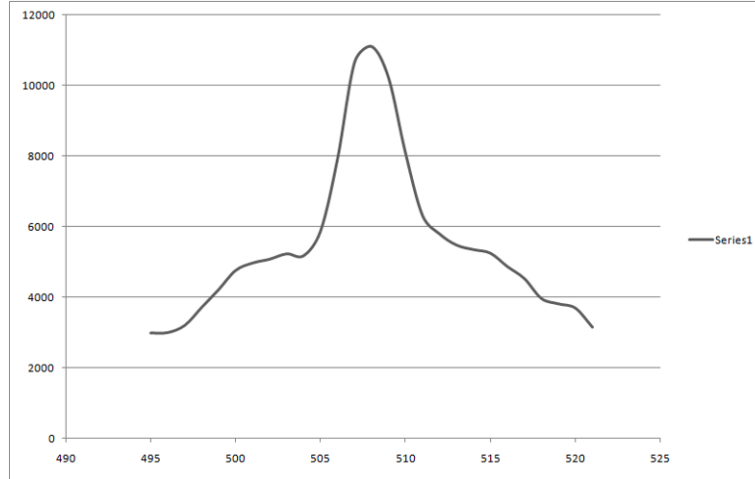


Fig. 21. This is a plot of the stacked $H\alpha$ images x -axis (E-W) values in y -axis (N-S) row 165 shown in Fig. 20 and Table 10.

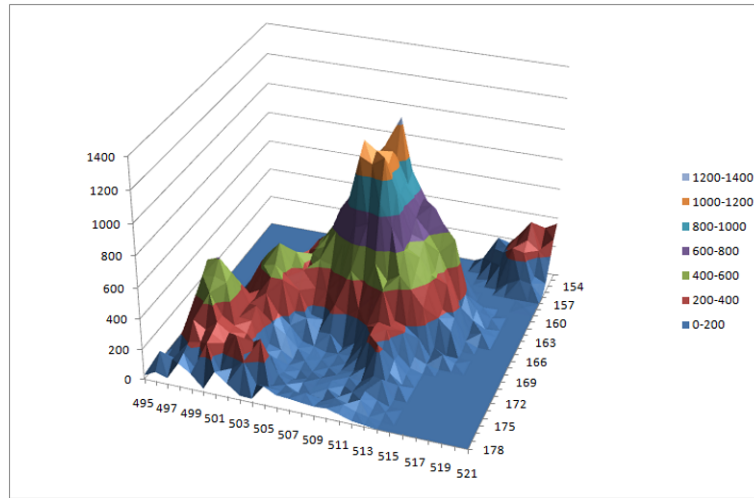


Fig. 22. This is a 27×27 pixel (110×110 pc) surface plot of the central SNR location of the stacked $[S II]$ images shown in Fig. 19. A plot of the peak along the x-axis (E-W) at y-axis (N-S) pixel row 165 is shown in Fig. 23.

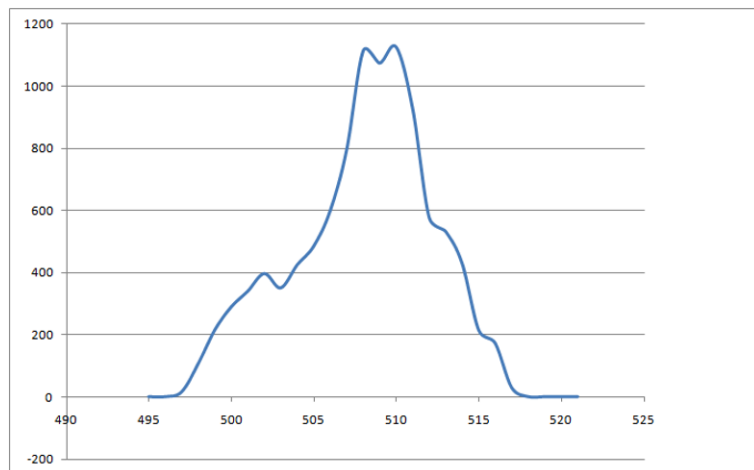


Fig. 23. This is a plot of the stacked $[S II]$ images x-axis values in y-axis row 165 shown in Fig. 22. The FWHM is taken at 550 counts as 7 pixels (28 pc).

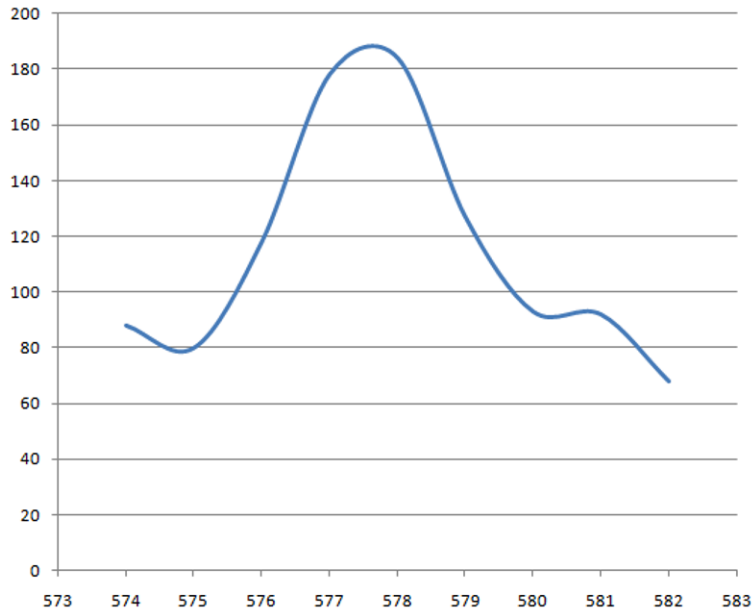


Fig. 24. This is the x-axis (E-W) emission profile of a small star from the [S II] J image. The FWHM is taken at 130 count with a pixel width of 3.7 (15 pc).

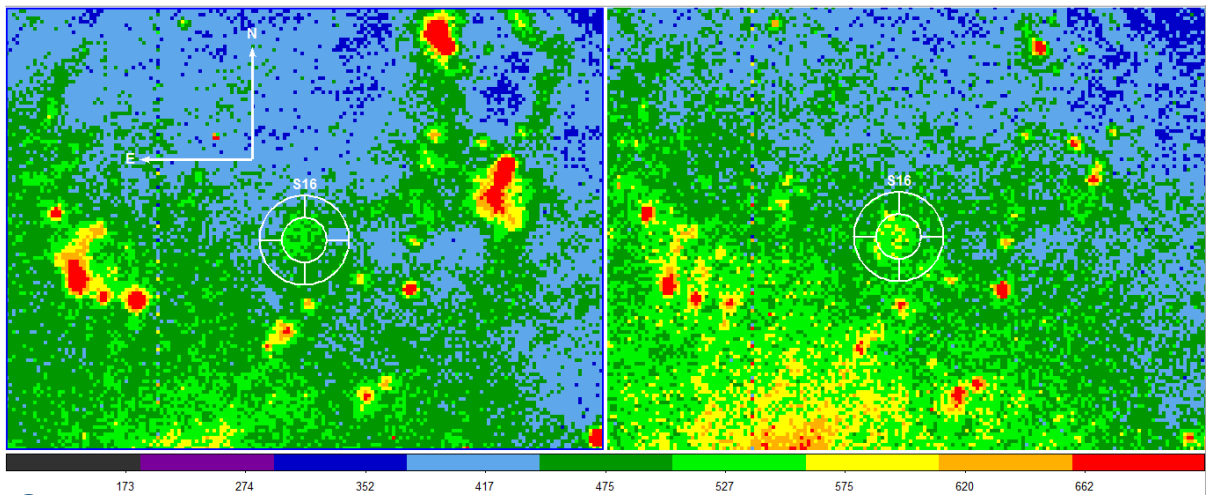


Fig. 25. This is the BL97 location of N300-S16 (α 00 54 54.46, δ -37 40 35.46) as found on the BL97 images (G) with 2MASS calibrated astrometry. The $H\alpha$ image is on the left and the [S II] image is on the right. The inner circle of the panda is 5".1 (52 pc) in diameter. The color scale is AIPS0, Zoom=4, Scale = ZScale, Squared.

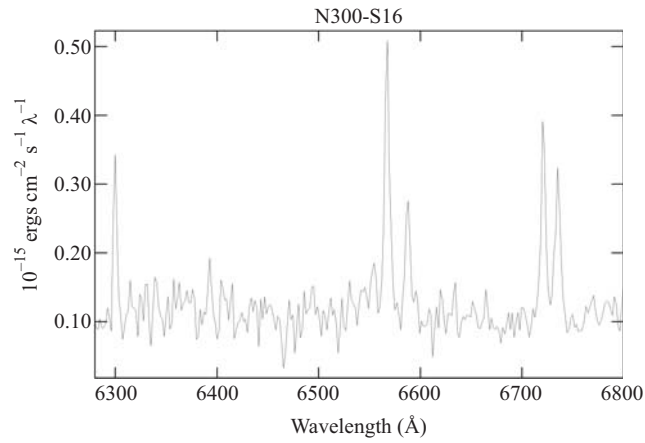


Fig. 26. *The spectrum of N300-S16 from MWF11. The spectrum also contains a strong [O I] line at 6300 \AA which is an indicator of shock fronts typical of SNRs. Note the broad band noise level in the spectrum and the low flux density.*

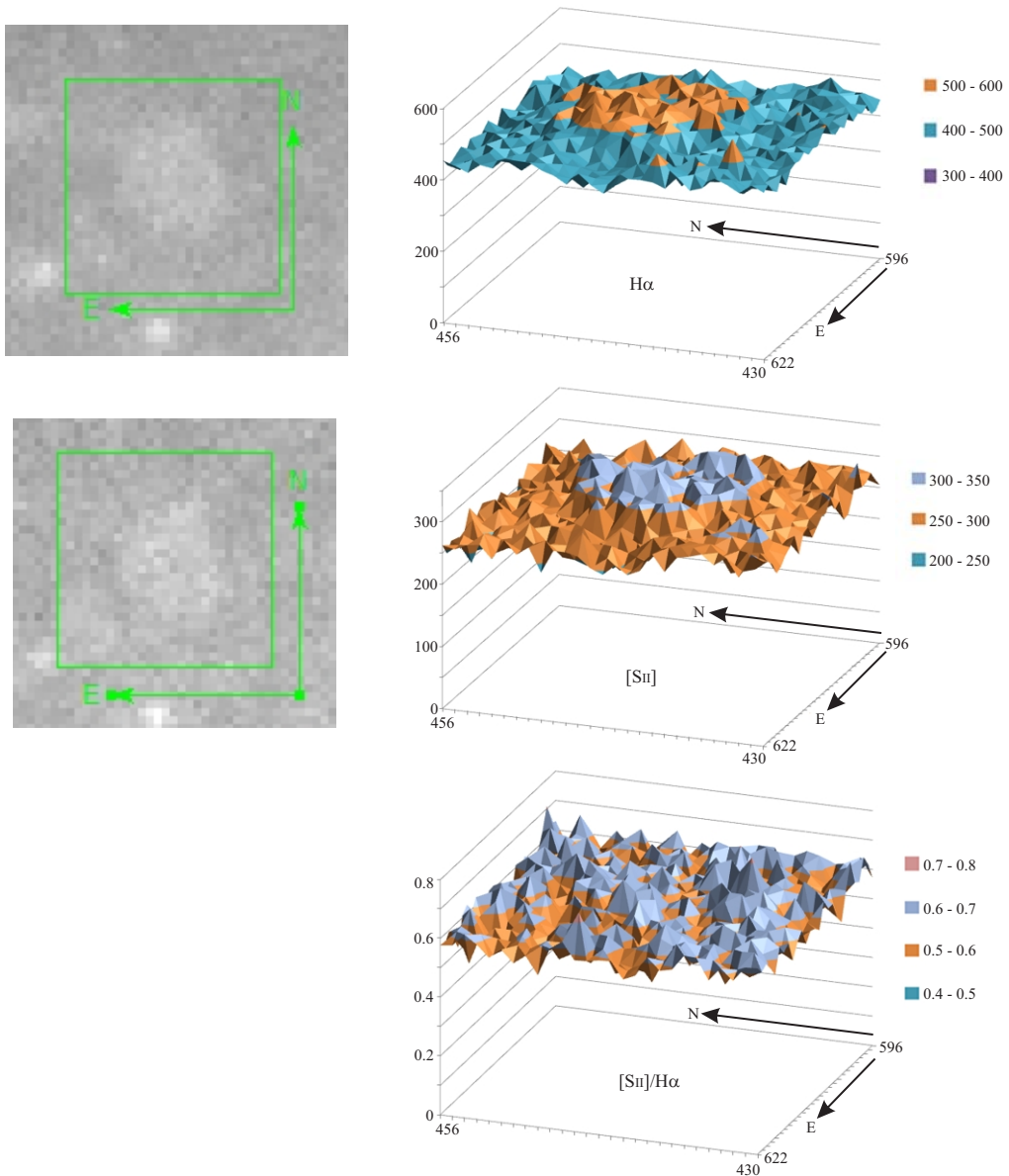


Fig. 27. These are 3-D plots of the BL97 image CCD pixel counts of N300-S16 in $H\alpha$ (top) and $[S II]$ (middle). The pixels plotted (a 27×27 array centered on the candidate's coordinates) are shown by the green box in the image tile on the left. The plot is shown on the right. In both cases the emissions are only slightly above the background but clear discernible. The size of the candidate implies it to be at the end of its PDS stage. The 3-D plot on the bottom was the result of dividing the $[S II]$ pixel value by the $H\alpha$ pixel value. The apparent SNR disappears in the high-level noise.